CHARACTERIZATIONS, ANTIGENICITY, AND IMMUNOGENICITY OF EXTRACELLULAR VESICLE PROTEINS FROM IRON-DEPRIVED *Mycolicibacterium smegmatis*

MEHALENE A/P JAYARAM

UNIVERSITI SAINS MALAYSIA

2025

CHARACTERIZATIONS, ANTIGENICITY, AND IMMUNOGENICITY OF EXTRACELLULAR VESICLE PROTEINS FROM IRON-DEPRIVED *Mycolicibacterium smegmatis*

by

MEHALENE A/P JAYARAM

Thesis submitted in fulfilment of the requirements
for the degree of
Doctor of Philosophy

September 2025

ACKNOWLEDGEMENT

With utmost devotion, I begin by expressing my heartfelt gratitude to my spiritual guru, Aanmiga Guru Arulthiru Bangaru Adigalar Amma, whose divine guidance and blessings have been my greatest source of strength and inspiration throughout this journey. I am deeply grateful to my supervisor, Dr. Norsyahida Arifin, for her dedicated guidance and support as well as to my co-supervisors, Dr. Maryam Azlan for her assistance with the immunogenicity studies in Kelantan, Associate Professor Dr. Nurulhasanah binti Othman for her valuable guidance and Dr Kye for giving me this project. My sincere thanks also go to Prof. Norazmi Mohd. Nor for funding some parts of my studies. I would like to acknowledge the academic and technical staff: En Masrul and Pn Faizah (EM Unit, SBS), Pn Nurul (Microbiology Lab, SBS), Kak Suhada (INFORMM), En Aiman (Oncology Unit, IPPT Bertam), En Mutalib (CGAR) and Dr. Nasuha (SBS) for their technical support. My appreciation also extends to ARASC Kelantan, Vaccinology and Immunology Team in Kelantan Kak Aifa, Hatimi, Dr. Syahida Ramli, Ain, Dr. Aini, Dr. Yon, MinXuan, and Kak Azirah, as well as my lab mates, Hamizah, Eiyad and Celine. Finally, I am deeply thankful to my parents, Sakthi Jayaram and Sakthi Rajasvari, my brothers, Tharmin Anne and Jenath Anne and my best friend, Sakthi Yaatha Varman, for their constant love, support and belief in me.

TABLE OF CONTENTS

ACKNOWLEDGEMENT ..... **ii**

TABLE OF CONTENTS ..... **iii**

LIST OF TABLES ..... **xi**

LIST OF FIGURES ..... **xii**

LIST OF SYMBOLS ..... **xvi**

LIST OF ABBREVIATIONS ..... **xviii**

LIST OF APPENDICES ..... **xxi**

ABSTRAK ..... **xxii**

ABSTRACT ..... **xxiv**

CHAPTER 1 INTRODUCTION **1**

1.1 Background of study 1

1.2 Statement of problem 2

1.3 Significance of the study and research questions 3

1.4 General Objective 3

1.4.1 Specific objectives of the study 4

CHAPTER 2 LITERATURE REVIEW **5**

2.1 Tuberculosis 5

2.2 Diagnosis of tuberculosis 5

2.3 Treatment of tuberculosis 6

2.4 BCG Vaccine for tuberculosis 8

2.4.1 BCG Vaccine effectiveness 12

2.4.2 Candidate vaccine against TB 12

2.5 Mycobacteria 13

2.5.1 *Mycolicibacterium smegmatis* 15

2.6 Extracellular vesicles 17

2.6.1 Extracellular vesicles isolation, characterization and stability..... 18

2.6.2 Mycobacteria EVs 24

2.6.3 Roles of iron in mycobacteria EVs 26

2.6.4 Functions of mycobacteria EVs 29

2.6.5 Proteomic analysis of mycobacteria EVs..... 30

2.6.6 Mycobacteria EVs as potential biomarkers and vaccination agents..... 33

2.6.7 Interaction of mycobacteria EVs with the immune system..... 34

2.6.8 Roles of IL-4 and IFN- γ cytokines in the immune response against EVs..... 35

CHAPTER 3 GENERAL MATERIALS AND METHODS 37

3.1 Study design 37

3.2 Materials and Methods 40

3.2.1 Mycobacteria strain 40

3.2.2 Serum samples and ethics 40

3.2.3 Chemicals and reagents 41

3.2.4 Antibodies and enzymes..... 41

3.3 Preparation of media and reagents for EV production 42

3.3.1 M7H9 broth and agar 42

3.3.2 Minimal media 42

3.3.3 Iron-depleted minimal medium 45

3.3.4 Stock solution of $ZnCl_2$, $MgSO_4$ and $MnSO_4$ 45

3.3.5 Sodium hydroxide and sodium chloride..... 46

3.4 Preparation of reagents for EVs isolation 46

3.4.1 Protease inhibitor..... 46

3.4.2 10mM Tris-HCl..... 46

3.4.3 Sodium azide for storage of column 47

3.5 Preparation of reagents for OFFGEL™ electrophoresis 47
3.5.1 OFFGEL™ stock solution 47
3.5.2 IPG strips rehydration solution 47
3.5.3 OFFGEL™ Protein solution 47
3.6 Preparation of reagents for SDS-PAGE. 47
3.6.1 Resolving gel buffer 47
3.6.2 Stacking gel buffer 48
3.6.3 SDS-Page separating and stacking gel 48
3.6.4 5× sample buffer 49
3.6.5 Ammonium persulfate 49
3.6.6 Running buffer 49
3.6.7 Staining solution 49
3.6.8 Destaining solution 49
3.7 Preparation of reagents for Western blot 50
3.7.1 Transfer buffer 50
3.7.2 Ponceau S staining 50
3.7.3 Washing and blocking solution 50
3.7.4 Primary and secondary antibodies 51
3.7.5 Chemiluminescence substrate 51
3.7.6 Fixer and developer 51
3.8 Preparation of reagents for ELISA 51
3.8.1 ELISA coating buffer 51
3.8.2 PBS-Tween 20 52
3.8.3 Blocking solution 52
3.8.4 Primary antibody and secondary antibody 52
3.8.5 ABTS Substrate solution 52
3.9 Preparation of reagents for in-gel digestion 53

3.9.1 Destaining solution 53
3.9.2 Reducing buffer 53
3.9.3 Alkylation buffer 53
3.9.4 Trypsin 53
3.9.5 Extraction solutions 53
3.10 Media for splenocyte culture 54
3.10.1 Media for splenocyte culture 55
3.11 Culture growth and centrifugation 55
3.11.1 Shaking culture 55
3.11.2 Stationary culture 56
3.11.3 Centrifugation 56
3.12 Preservation and storage 57

CHAPTER 4 PRODUCTION, ISOLATION, AND STABILITY OF EXTRACELLULAR VESICLES OF *Mycolicibacterium smegmatis* 58

4.1 Introduction 58
4.2 Methodology 59
4.2.1 Optimizing incubation duration and culture media 59
4.2.2 Growing MSMEG in iron-depleted conditions 61
4.2.3 Determination of EV stability 64
4.2.3(a) Nanoparticle tracking analysis (NTA) 64
4.2.3(b) TEM observation 64
4.2.3(c) Protein quantification 65
4.2.3(d) SDS-PAGE and Western blot analysis 66
4.3 Results 68
4.3.1 Optimizing MSMEG culture duration and culture media. 68
4.3.2 Growing MSMEG in iron-depleted conditions 72
4.3.3 Collection and isolation of EV and confirmation by TEM 74

4.3.4 Determining EVs stability 77
4.3.4(a) Nanoparticle tracking analysis (NTA) 77
4.3.4(b) TEM observation 78
4.3.4(c) EVs protein quantification 80
4.3.4(d) Western blot analysis 83
4.4 Discussion 86
4.5 Conclusion 96

CHAPTER 5 EVALUATION OF THE ANTIGENICITY OF MSMEG EVs.. 97

5.1 Introduction 97
5.2 Methodology 98
5.2.1 Serum characterization 98
5.2.2 Antigen preparation 98
5.2.3 ELISA 99
5.2.4 OFFGEL^{TM} Electrophoresis 101
5.2.5 SDS-PAGE and Coomassie Blue staining 102
5.2.6 Western blot analysis 102
5.2.6(a) Blocking buffer optimization 102
5.2.6(b) Secondary antibody concentration optimization 103
5.2.6(c) Combined optimization of serum and secondary antibody 103
5.2.6(d) Western blot of OFFGEL fractions under optimized conditions 103
5.2.7 Proteomic analysis 104
5.2.7(a) In-gel digestion 104
5.2.7(b) Mass spectrometry analysis 105
5.3 Results 106
5.3.1 ELISA 106

5.3.2 OFFGEL^{TM} electrophoresis 108

5.3.3 Western blot analysis 110

5.3.3(a) Blocking buffer optimization 110

5.3.3(b) Secondary antibody concentration optimization 111

5.3.3(c) Combined optimization of serum and secondary antibody 112

5.3.3(d) Western blot of OFFGEL fractions under optimized conditions 114

5.3.4 Proteomic analysis 116

5.3.4(a) In-gel digestion 116

5.3.4(b) Mass spectrometry analysis 117

5.4 Discussion 119

5.5 Conclusion 123

CHAPTER 6 IMMUNOGENICITY OF MSMEG EVs IN MICE 125

6.1 Introduction 125

6.2 Methodology 126

6.2.1 Optimization of EV preparation for mice immunization 126

6.2.1(a) EVs production and quantification method 126

6.2.1(b) Mice handling 127

6.2.1(c) EVs concentration optimization for mice immunization 128

6.2.1(d) Blood collection from mice 128

6.2.1(e) Mice immunization 129

6.2.1(f) Splenocyte preparation and cell concentration determination 130

6.2.1(g) Flow cytometry cell preparation and EV stimulation optimization 131

6.2.1(h) Flow cytometry 132

6.2.2 Immunization of mice after MSMEG EVs concentration optimization 134

6.2.2(a) BCG preparation 134

6.2.2(b) EVs + alum preparation 134

6.2.2(c) Mice handling and mice immunization 134

6.2.3 Enzyme-linked immunosorbent assay (ELISA) 137

6.2.3(a) Checkerboard titration for antigen and serum optimization 137

6.2.3(b) ELISA using individual mice sera 139

6.2.4 Statistical analysis 140

6.3 Results 141

6.3.1 Optimization of EV preparation for mice immunization 141

6.3.1(a) EV quantification method 141

6.3.1(b) EVs concentration optimization for mice immunization and splenocyte stimulation 143

6.3.1(c) Flow cytometry gating strategy 143

6.3.1(d) Flow cytometry results for EV concentration optimization 146

6.3.2 Evaluation of physiological response in mice post-immunization 149

6.3.2(a) Weekly mice body weight 149

6.3.3 Evaluation of cellular immune response in mice post-immunization 150

6.3.3(a) Lymphocyte viability 150

6.3.3(b) Expression of activation markers 151

6.3.3(c) Expression of memory markers 153

6.3.3(d) Intracellular cytokine production 155

6.3.4 Evaluation of humoral immune response in mice post-immunization 161

6.3.4(a) ELISA 161

6.4 Discussion 163

6.5 Conclusion 172

CHAPTER 7 GENERAL DISCUSSION, CONCLUSION AND FUTURE RESEARCH 173

7.1 General discussion 173

7.2 Conclusion 176

7.3 Recommendation for future research 177

REFERENCES 179

APPENDICES

LIST OF PUBLICATIONS

LIST OF TABLES

Page

Table 2.1 Summary of immune responses generated after BCG administration....10

Table 2.2 Summary of EVs isolation techniques, advantages and limitations ..20

Table 2.3 Summary of EVs characterization techniques, advantages and limitations....22

Table 2.4 List of *M. bovis*, *M. tuberculosis* and *M. smegmatis* EV proteins from literature....32

Table 3.1 List of antibodies, enzymes and the sources 41

Table 3.2 Composition of minimal media used for EV production optimization 44

Table 3.3 Composition of various iron-depleted media....45

Table 3.4 Recipe for 10% SDS-Page 48

Table 4.1 MSMEG culture conditions and presence of EVs (SEM/TEM) observation 76

Table 4.2 NTA results of MSMEG EVs under different storage conditions 78

Table 4.3 Protein concentration of EVs determined by Nanodrop 82

Table 5.1 Optimization of antigen and antibody concentrations by checkerboard ELISA 106

Table 5.2 Identification of potential immunogenic MSMEG EV proteins from crude EVs and fraction 6 118

Table 6.1 Mass of lyophilized EVs with 50mM trehalose....141

Table 6.2 Mass of lyophilized 50mM trehalose....142

LIST OF FIGURES

Page

Figure 2.1 The immune responses after intradermal BCG injection. 9

Figure 2.2 Transmission electron microscopy images of MTB EVs 26

Figure 2.3 An illustration of the roles of iron in MTB EVs 28

Figure 2.4 Venn diagram illustrates the shared and unique EV proteins among *M. tuberculosis*, *M. bovis* and *M. smegmatis.* 33

Figure 3.1 Flow chart of study 39

Figure 3.2 General mice immunization procedure 55

Figure 4.1 Flow chart of EV isolation and confirmation methods 60

Figure 4.2 Workflow for MSMEG EV production in iron-depleted minimal medium 63

Figure 4.3 SEM analysis of MSMEG grown in Media 1 to assess EV production over time 69

Figure 4.4 TEM analysis of negatively stained pellet from MSMEG grown in Media 1 for 4 days 70

Figure 4.5 SEM analysis of MSMEG grown in Media 2-8 for 4 days to identify optimal media for EV production 71

Figure 4.6 SEM analysis of MSMEG grown in the iron-depleted minimal medium for different durations for EV production 73

Figure 4.7 SEM analysis of MSMEG grown in various iron-depleted minimal medium for EV production 74

Figure 4.8 TEM confirmation of harvested MSMEG EVs 75

Figure 4.9 TEM analysis of the morphology of MSMEG EVs incubated under various conditions 79

Figure 4.10 BSA standard curve for protein quantification using RC-DC™ Protein Assay 80

Figure 4.11 Nanodrop measurement of protein concentration of EVs stored at various conditions 82

Figure 4.12 Western blot analysis of Ag85 in MSMEG EVs after short term storage 84

Figure 4.13 Western blot analysis of Ag85 in MSMEG EVs after storage for one month 85

Figure 5.1 Checkerboard titration plate design layout for IgG ELISA optimization using human sera 100

Figure 5.2 ELISA plate color development after ABTS substrate addition 107

Figure 5.3 Scatter plot of ELISA results comparing IgG antibody responses between TB+ sera and TB-human sera 108

Figure 5.4 The protein profile of MSMEG EVs from OFFGEL fractionation stained with Coomassie Blue 109

Figure 5.5 Western blot analysis of blocking buffer optimization using sonicated crude MSMEG EVs. 111

Figure 5.6 Western blot analysis for secondary antibody dilution optimization using sonicated crude MSMEG EVs 112

Figure 5.7 Western blot analysis for combined patient sera (PAB) and secondary antibody (SAB) optimization using sonicated crude MSMEG EVs. 113

Figure 5.8 Western blot analysis of MSMEG EVs OFFGEL fractions 115

Figure 5.9 Coomassie Blue stained SDS-PAGE of crude MSMEG EVs and OFFGEL fraction 6. 116

Figure 6.1 Procedure for blood and spleen isolation from mice 129

Figure 6.2 Illustration of mice immunization, blood and spleen collection durations according to groups 136

Figure 6.3 Checkerboard titration plate design layout for IgG ELISA optimization 138

Figure 6.4 EVs particle size ranges determined with NTA 143

Figure 6.5 Gating strategy plots for flow cytometry analysis of mice splenocytes 145

Figure 6.6 The expression of $CD69^+$ by $CD4^+$ T cells from mice immunized and stimulated with different concentrations of MSMEG EVs 146

Figure 6.7 The expression of $CD62L^+$ by $CD4^+$ T cells from mice immunized and stimulated with different concentrations of MSMEG EVs 147

Figure 6.8 The expression of IL-4^+ and IFN-γ^+ cytokines produced by $CD4^+$ T cells from mice immunized and splenocytes stimulated with different concentrations of MSMEG EVs. 148

Figure 6.9 Weekly mice body weight from different immunization groups 149

Figure 6.10 Lymphocyte cell viability after 72 hours of incubation with or without stimulation 150

Figure 6.11 The expression of $CD69^+$ by $CD4^+$ T cells in the spleen of vaccinated mice 151

Figure 6.12 The expression of $CD8^+CD69^+$ in splenocytes of mice stimulated with MSMEG EVs. 152

Figure 6.13 The expression of $CD62L^+$ by $CD4^+$ T cells in the spleen of vaccinated mice. 153

Figure 6.14 The expression of $CD62L^+$ by $CD8^+$ T cells in the spleen of vaccinated mice. 154

Figure 6.15 The production of $CD4^+$IFN-γ^+ in lymphocytes of mice stimulated with MSMEG EVs 155

Figure 6.16 The production of $CD8^+$IFN-γ^+ in lymphocytes of mice stimulated with MSMEG EVs 156

Figure 6.17 The production of $CD4^+$IL-4^+ in lymphocytes of mice stimulated with MSMEG EVs 157

Figure 6.18 The production of $CD8^+$ IL-4^+ T cell in lymphocytes of mice stimulated with MSMEG EVs. 158

Figure 6.19 Comparison of IFN-γ^+ and IL-4^+ cytokine production in T cells from different mice groups 160

Figure 6.20 Checkerboard ELISA to optimize antigen coating and antibody dilutions using sera from vaccinated mice. 161

Figure 6.21 IgG antibody responses against MTB H37Rv WCL and MSMEG EVs in vaccinated mice 162

LIST OF SYMBOLS

%	Percent
g/L	Grams per liter
:	Ratio
<	Less than
±	Plus-minus
°	Degree
°C	Degrees Celsius
µg	Microgram
µg/mL	Micrograms per milliliter
µL	Microliter
µm	Micrometer
et al.	*et alia* (Latin for "and others")
g	Gram
hz	Hertz (frequency, cycles per second)
kDa	Kilodalton
kV	Kilovolt
L	Liter
M	Molar (mol/L; concentration)
mA	Milliampere
mg	Milligram
mg/L	Milligrams per liter
mg/mL	Milligrams per milliliter
mL	Milliliter
mM	Millimolar
mm	Millimeter

ng/mL	Nanograms per milliliter
nm	Nanometer
p	Probability value (in statistics)
pH	Potential of Hydrogen (acidity/alkalinity measure)
rpm	Revolutions per minute
V	Volt
W/W	Weight by weight
×g	relative centrifugal force (RCF)

LIST OF ABBREVIATIONS

ABTS	2,2'-Azino-bis(3-ethylbenzothiazoline-6-sulfonic acid)
ACK	Ammonium-Chloride-Potassium
ACN	Acetonitrile
ADC	Albumin Dextrose Catalase
ADH	Alcohol Dehydrogenase
AG85	Antigen 85 complex
AIDS	Acquired Immunodeficiency Syndrome
ANOVA	Analysis of Variance
APS	Ammonium Persulfate
ATCC	American Type Culture Collection
ATP	Adenosine Triphosphate
BCG	Bacillus Calmette-Guérin
BSA	Bovine Serum Albumin
$C_4H_8N_2O_3.H_20$	L-Asparagine monohydrate
$C_6HSO_7.Fe.NH_3$	Ferric ammonium citrate
$CaCl_2$	Calcium Chloride
CFU	Colony-Forming Unit
CO_2	Carbon Dioxide
ConA	Concanavalin A
CST	Cell Signaling Technology
dH_20	Distilled Water
DNA	Deoxyribonucleic Acid
DTT	Dithiothreitol
ECL	Enhanced Chemiluminescence
EDTA	Ethylenediaminetetraacetic Acid
ELISA	Enzyme-Linked Immunosorbent Assay
EPS	Extracellular Polymeric Substance
EVs	Extracellular Vesicles
FACS	Fluorescence-Activated Cell Sorting
FBS	Fetal Bovine Serum
FESEM	Field Emission Scanning Electron Microscopy

FSC-A	Forward Scatter Area
FSC-H	Forward Scatter Height
FVS780	Fixable Viability Stain 780
HCL	Hydrochloric Acid
HIV	Human Immunodeficiency Virus
HMDS	Hexamethyldisilazane
HRP	Horseradish Peroxidase
IFN-γ	Interferon Gamma
IgG	Immunoglobulin G
IGRA	Interferon-Gamma Release Assay
IL-4	Interleukin 4
IPG	Immobilized pH Gradient
KH_2PO_4	Potassium Dihydrogen Phosphate
LAM	Lipoarabinomannan
LTBI	Latent Tuberculosis Infection
$MgSO_4$	Magnesium Sulfate
MHC I	Major Histocompatibility Complex Class I
miRNA	MicroRNA
MISEV	Minimal Information for Studies of Extracellular Vesicles
MM	Minimal Medium
$MnSO_4$	Manganese Sulfate
mRNA	Messenger Ribonucleic Acid
MSMEG	*Mycolicibacterium* smegmatis
MTB	*Mycobacterium tuberculosis*
MTB/RIF	*Mycobacterium tuberculosis*/Rifampicin resistance
MTB/XDR	*Mycobacterium tuberculosis*/Extensively Drug-Resistant
MWCO	Molecular Weight Cut-Off
Na_2HPO_4	Disodium Hydrogen Phosphate
NADP	Nicotinamide Adenine Dinucleotide Phosphate
NaOH	Sodium Hydroxide
NTA	Nanoparticle Tracking Analysis
NTM	Nontuberculous Mycobacteria
OADC	Oleic Acid-Albumin-Dextrose-Catalase
OD	Optical Density

PBS	Phosphate-Buffered Saline
PBST	PBS with Tween-20
PPD	Purified Protein Derivative
PQS	Pseudomonas Quinolone Signal
PRR	Pattern Recognition Receptor
QTOF LC/MS	Quadrupole Time-of-Flight Liquid Chromatography/Mass Spectrometry
ROS/RNI	Reactive Oxygen Species / Reactive Nitrogen Intermediates
RPMI	Roswell Park Memorial Institute (medium)
RT	Room Temperature
SDS	Sodium Dodecyl Sulfate
SDS-PAGE	SDS-Polyacrylamide Gel Electrophoresis
SE	Standard Error of the Mean
SEM	Scanning electron microscope
SSC-A	Side Scatter Area
TB	Tuberculosis
TB+	Sera from TB patients
TB-	Sera from non-TB patients
TBS	Tris-Buffered Saline
TBST	TBS with Tween-20
TEM	Transmission Electron Microscopy
TEMED	Tetramethylethylenediamine
TFA	Trifluoroacetic Acid
TLR	Toll-Like Receptor
TST	Tuberculin Skin Test
WCL	Whole Cell Lysate
WHO	World Health Organization
ZN	Ziehl–Neelsen stain
$ZnCl_2$	Zinc Chloride
$ZnSO_4$	Zinc Sulfate

LIST OF APPENDICES

Appendix A	FIND VIETNAM Serum samples
Appendix B	JEPem-USM Ethics Approval
Appendix C	JKPPH-USM Ethics Approval
Appendix D	List of chemicals, reagents and the sources
Appendix E	NTA results of stability and mice immunization studies
Appendix F	Statistical analysis of ELISA using TB+ and TB- patient sera
Appendix G	LC-MS/MS results
Appendix H	Statistical analysis of flow cytometry
Appendix I	Statistical analysis of IgG ELISA using mice sera

PENCIRIAN, ANTIGENISITI, DAN IMMUNOGENISITI PROTEIN VESIKEL EKSTRASEL DARIPADA *Mycolicibacterium smegmatis* KEKURANGAN ZAT BESI

ABSTRAK

Tuberkulosis (TB), pembunuh berjangkit utama di dunia, kekal sebagai cabaran terbesar dalam kesihatan global. Vaksin BCG, satu-satunya vaksin yang tersedia, memberikan perlindungan terhad yang berkurangan dari semasa ke semasa. Vesikel ekstrasel (EV) daripada *Mycobacteria tuberculosis* (MTB) telah menunjukkan potensi sebagai vaksin TB, tetapi pengasingannya terhad disebabkan oleh kadar pertumbuhan MTB yang perlahan dan risiko bahaya biologi. Kajian ini menggunakan *Mycolicibacterium smegmatis* (MSMEG), organisma model yang pantas membiak dan tidak patogenik, untuk menghasilkan EV di bawah keadaan kekurangan zat besi. EV ini dinilai dari segi kestabilan, keantigenan menggunakan tiga sera pesakit TB positif yang digabungkan, serta potensinya sebagai penggalak vaksin BCG dalam tikus. EV yang diliofilisasi mengekalkan keantigenan dan kestabilan struktur, seperti yang disahkan melalui analisis penjejakan nanopartikel, mikroskop elektron transmisi dan pengujian Western blot. Elektroforesis OFFGEL^{TM} membolehkan pengasingan protein EV yang lebih baik, membolehkan pengesanan protein 46 kDa alkohol dehidrogenase (ADH), yang antigenik dalam sera pesakit TB. ADH daripada EV MSMEG berpotensi sebagai sasaran terapeutik dalam rawatan jangkitan MTB, berdasarkan peranannya dalam sintesis dinding sel dan pembentukan biofilm. Kajian immunogenisiti dalam tikus menunjukkan bahawa gabungan BCG+EVs meningkatkan sel T memori efektor $CD4^{+}$, seperti yang ditunjukkan oleh ekspresi CD62L yang rendah (21.48% ± 1.08) berbanding BCG (70.35% ± 2.26, $p < 0.0001$).

Gabungan BCG+EVs juga menurunkan paras IL-4^+ (0.10% ± 0.02) berbanding BCG (4.41% ± 0.49, $p < 0.0001$). Immunisasi EVs sahaja menghasilkan tahap IFN-γ^+ yang tertinggi (1.73% ± 0.28 $p < 0.0001$) manakala gabungan BCG+EVs mengekalkan tahap IFN-γ^+ yang setara dengan BCG (0.52% ± 0.09 berbanding 0.52% ± 0.06 $p < 0.0001$) dan menurunkan paras IL-4^+, menunjukkan tindak balas imun jenis Th1. Penemuan ini menunjukkan bahawa EV MSMEG adalah stabil, imunogenik dan menawarkan alternatif yang lebih selamat dan boleh diskala berbanding komponen yang berasal daripada MTB untuk pembangunan vaksin TB.

CHARACTERIZATIONS, ANTIGENICITY, AND IMMUNOGENICITY OF EXTRACELLULAR VESICLE PROTEINS FROM IRON-DEPRIVED *Mycolicibacterium smegmatis*

ABSTRACT

Tuberculosis (TB), the world's leading infectious killer, remains a major global health challenge. BCG, the only available vaccine, provides limited protection that wanes over time. Extracellular vesicles (EVs) from *Mycobacterium tuberculosis* (MTB) have shown vaccine potential, but their isolation is hindered by slow bacterial growth and biohazard risks. This study used *Mycolicibacterium smegmatis* (MSMEG), a fast-growing, non-pathogenic model organism, to produce EVs under iron-depleted conditions. These EVs were evaluated for stability, antigenicity using three pooled TB positive patient sera and their potential as a BCG booster vaccine in mice. Lyophilized EVs maintained antigenicity and structural stability, as confirmed by nanoparticle tracking analysis, transmission electron microscopy and western blotting. OFFGEL^{TM} electrophoresis enabled improved EV protein separation, allowing for the identification of the antigenic 46 kDa iron-containing alcohol dehydrogenase (ADH) protein. Given its role in cell wall synthesis and biofilm formation, ADH from MSMEG EVs represents a promising therapeutic target against MTB infections. Immunogenicity studies in mice revealed that the BCG+EVs booster increased the frequency of $CD4^+$ effector memory T cells, as indicated by lower CD62L expression (21.48% ± 1.08) compared to BCG alone (70.35% ± 2.26, $p < 0.0001$). The BCG+EVs booster also reduced IL-4^+ levels (0.10% ± 0.02) vs BCG (4.41% ± 0.49, $p < 0.0001$). EVs given alone induced the highest IFN-γ^+ levels (1.73% ± 0.28) while the BCG+EVs booster maintained similar IFN-γ^+ levels to BCG alone (0.52% ± 0.09 vs

0.52% ± 0.06) and suppressed IL-4^{+} levels indicating a Th1-type immune response. These findings highlight that MSMEG EVs are stable, immunogenic and offer a safer, scalable alternative to MTB-derived components for TB vaccine development.

CHAPTER 1

INTRODUCTION

1.1 Background of study

Tuberculosis caused primarily by MTB, remains a major global health challenge (Chiaradia et al., 2017; Cheng & Schorey, 2019). Although the Bacillus Calmette–Guérin (BCG) vaccine is widely used, its protective efficacy against pulmonary TB in adolescents and adults is limited (Fatima et al., 2020; Kaufmann, 2021). Consequently, mycobacteria EVs have emerged as a promising avenue for developing novel strategies to enhance immunity against TB (Prados-Rosales et al., 2014b).

EVs are nanosized, membrane-bound particles secreted by bacteria that carry proteins, lipids and nucleic acids (Welsh et al., 2024). In MTB, EVs have been shown to modulate immune responses and interact with host cells, with EV-associated proteins capable of stimulating T cell responses (Prados-Rosales et al., 2014b; Athman et al., 2015; Gupta & Rodriguez, 2018). EVs also reflect the physiological state of the bacteria, particularly under environmental stresses such as iron limitation, which is encountered during infection and can influence EV production and cargo composition (Prados-Rosales et al., 2014a; Gupta & Rodriguez, 2018; Gupta & Rodriguez, 2019; Welsh et al., 2024).

Although administration of MTB EVs after BCG immunization enhances immune responses, demonstrating their vaccine potential (Prados-Rosales et al., 2014b; Salgueiro et al., 2024), their use is limited by safety concerns and compositional heterogeneity, which can lead to inconsistent protection. Moreover,

pathogenic EVs such as MTB and BCG EVs may be detrimental to the host during infection (Prados-Rosales et al., 2011). While MTB EVs have been extensively studied, relatively little is known about EVs produced by non-tuberculous mycobacteria such as MSMEG (Prados-Rosales et al., 2011). MSMEG is a fast-growing, non-pathogenic species that shares extensive genetic and physiological similarities with MTB, including conserved metabolic pathways and cell wall structure, making it a safer and suitable model for studying mycobacterial EVs (Sparks et al., 2023). Notably, in MTB-challenged mice, treatment with MSMEG EVs resulted in lower bacterial loads in the lungs compared to PBS or BCG EVs, suggesting a potential host-beneficial effect (Prados-Rosales et al., 2011).

However, the immunological properties of MSMEG EVs, especially under biofilm growth or iron-limited conditions, remain poorly understood. Studying these features could reveal their potential to modulate host immunity and guide safer EV-based TB vaccination strategies.

1.2 Statement of problems

The protective efficacy of the TB vaccine, BCG wanes over time (Fatima et al., 2020). While potential TB vaccines from MTB EVs have been reported (Prados-Rosales et al., 2014b), isolating these EVs poses significant challenges due to the slow growth rate, variable yields depending on culture conditions (Gupta & Rodriguez, 2019; Schirmer et al., 2022), high biohazard levels (Salgueiro et al., 2024) and the risk of promoting TB dissemination (Prados-Rosales et al., 2011; Athman et al., 2015; Gupta & Rodriguez, 2018).

1.3 Significance of the study and research questions

This study aims to complement existing vaccines by identifying antigenic proteins in MSMEG EVs that may play a role in immune activation. Additionally, this study aims to determine the immunogenicity of the EVs in mice to evaluate their potential as BCG boosters. These findings have the potential to enhance vaccine efficacy and strengthen public health initiatives aimed at controlling the spread of tuberculosis.

Research questions

Based on the promising applications of EVs in vaccine development and therapeutic interventions, this study seeks to evaluate the potential of MSMEG, a non-pathogenic and fast-growing species, as a model organism. By focusing on the antigenicity of MSMEG EVs when exposed to tuberculosis patient sera and examining their potential as a BCG booster vaccine, this research endeavors to answer the following questions:

1. Can MSMEG, a non-pathogenic fast-growing species serve as an effective model organism to evaluate the antigenicity of MSMEG EVs using tuberculosis patient sera?
2. What is the potential of MSMEG EVs to serve as a booster vaccine that enhances the efficacy of the BCG vaccine in preventing tuberculosis?

1.4 General objective

To characterize EV proteins from iron-deprived MSMEG and evaluate their antigenic and immunogenic properties.

1.4.1 Specific objectives of the study

1. To produce and isolate MSMEG EVs
2. To assess the stability of MSMEG EVs under various storage temperatures and durations.
3. To evaluate the antigenicity of MSMEG EVs using TB and non-TB patient sera.
4. To evaluate the immunogenicity of MSMEG EVs in mice.

CHAPTER 2

LITERATURE REVIEW

2.1 Tuberculosis

MTB is the causative agent of tuberculosis which has plagued humankind since ancient times (Chiaradia et al., 2017; Cheng & Schorey, 2019). Inhalation of droplet nuclei of respiratory secretion containing tubercle bacilli can result in tuberculosis if the immune system fails to destroy the bacilli (Alsayed & Gunosewoyo, 2023). Despite advancements in medicine, tuberculosis remains one of the deadliest infectious diseases, claiming over 1.2 million lives worldwide in 2023, including 161,000 people with HIV. Additionally, an estimated 10.8 million people have fallen ill with TB in 2023 (World Health Organization, 2024).

TB mainly affects the lung (pulmonary TB) but can also spread to other sites of the body (extrapulmonary TB) (Alsayed & Gunosewoyo, 2023). The disease affects low- and middle-income countries such as India, Indonesia, China, Philippines, Pakistan, Nigeria, Bangladesh and Congo accounting for the highest TB burden (World Health Organization, 2024a). Of the people who developed TB in 2023, 55% were men, followed by 33% women, and 12% children.

In Malaysia, notably, the state of Sabah has reported 20-30% of the total TB cases in the country (Goroh et al., 2020).

2.2 Diagnosis of tuberculosis

Despite global TB elimination strategies, several factors hinder disease control. Early and accurate diagnosis of TB is important to prevent the spread of MTB. Several diagnostic techniques exist, such as immunological, radiographical, microscopical,

bacteria culture and clinical approaches (Alsayed & Gunosewoyo, 2023). These technologies endorsed by WHO are grouped into two categories that are direct detection and indirect detection. Direct detection involves detecting the mycobacteria itself through methods such as microscopy, culture and molecular tests such as GeneXpert. In contrast, indirect detection focuses on detecting the immune response against the MTB using tests such as the tuberculin skin test and interferon-gamma release assays (Oommen & Banaji, 2017).

The basic and direct TB diagnostic method is sputum smear microscopy using Ziehl-Neelsen (ZN) staining method. This method uses carbol-fuchsin that stains the mycobacteria after gentle heating, while non-mycobacterial bacilli are decolorized using acid that removes the excess stains. Consequently, mycobacteria strains appear red and methylene blue serves as a counterstain for better visualization. While this method is economical, simple and rapid, it cannot differentiate between live and dead bacteria, limiting its diagnostic accuracy (Heemskerk et al., 2015; Oommen & Banaji, 2017). Despite the slow replication time of MTB, culture methods remain the gold standard for TB diagnosis. MTB forms visible colonies after 4-6 weeks on solid media (Lowenstein-Jensen, Ogawa, Middlebrook 7H10/11agar) and 10-21 days in liquid broth (Middlebrook 7H9) (Heemskerk et al., 2015).

Each detection has its strengths and limitations, and the choice of a test depends on the resources, time, diagnostic needs and patient populations.

2.3 Treatment of tuberculosis

The treatment of TB is based on a prolonged regimen of combination therapy to ensure bacterial eradication and drug resistance prevention. The global standard for drug-susceptible tuberculosis treatment consists of an intensive 2-month phase of

using rifampicin, isoniazid and pyrazinamide, followed by a 4-month continuation phase with rifampicin and isoniazid. This regimen could cure most patients with drug-susceptible TB (Motta et al., 2024). However, drug-resistant TB remains a significant challenge. The most prevalent form of MTB resistance worldwide is the isoniazid resistance without concurrent rifampicin resistance. The WHO recommends a 6-month regimen of ethambutol, pyrazinamide, rifampicin and levofloxacin to treat isoniazid-resistant, rifampicin-susceptible TB (Tahseen et al., 2020). Treatment regimens and duration vary for other types of multidrug-resistant tuberculosis (Motta et al., 2024).

TB treatment involves anti-tuberculosis drugs that are classified into first-line, second-line and third-line drugs. Isoniazid, rifampicin, pyrazinamide, streptomycin and ethambutol are first-line drugs that are highly effective with low toxicity, killing active bacteria during the early stages of infection. Second-line drugs such as cycloserine, ethionamide, aminoglycosides and fluoroquinolones are less effective and more toxic, inhibiting bacterial growth and strengthening treatment effectiveness against resistant strains. Third-line antibiotics are given to patients suffering from extensively drug-resistant tuberculosis (Chauhan et al., 2021; Bhanu, 2023).

Most of the anti-mycobacterial drugs either inhibit protein or cell wall synthesis of MTB leading to MTB death (Bhanu, 2023). For example, rifampicin blocks the messenger RNA elongation by binding to the β-subunit of RNA polymerase whereas streptomycin inhibits MTB protein synthesis by binding to the 30S ribosomal subunit, disrupting the initiation of translation. Besides that, isoniazid inhibits mycolic acid synthesis, disrupting the MTB cell wall, whereas pyrazinamide through the enzyme pyrazinamidase disrupts bacteria membrane function, inhibiting fatty acid synthesis and leading to MTB cell damage. On the other hand, ethambutol prevents MTB from multiplying by inhibiting the synthesis of arabinogalactan in the cell wall

(Palomino & Martin, 2014; Bhanu, 2023). Despite existing therapies, TB treatments remain challenging due to prolonged drug regimens and emerging drug resistance. The development of shorter, more effective and less toxic regimens such as those incorporating bedaquiline, may show promising results in reducing treatment duration in both drug-susceptible and drug-resistant TB (Motta et al., 2024).

2.4 BCG Vaccine for tuberculosis

Bacille Calmette-Guérin (BCG) is the sole vaccine for TB prevention over the past 100 years (Kaufmann, 2021). BCG was created by passaging *Mycobacterium bovis* until it could not cause disease in healthy individuals, making it a suitable vaccine for MTB. Different BCG strains have emerged from genetic changes over time during its propagation worldwide and their effectiveness in inducing immune responses may vary. BCG is affordable and widely available with high safety across all age groups except in HIV-positive and immune-compromised individuals (Ahmed et al., 2021).

Intradermal BCG vaccination administration is recognized by several pattern recognition receptors (PRRs) present on neutrophils, monocytes, macrophages and dendritic cells, thus initiating the immune response (Ahmed et al., 2021). The live BCG persists at the site of injection for 2-4 weeks, with early responses from neutrophils. Neutrophils generate ROS/RNI response whereas macrophages, dendritic cells and neutrophils secrete IL-6, TNF-α, MIP-1α, MIP-1β, IL-8, IL-1α, IL-10, IL-4. These innate mediators are released within 1-3 hours after BCG vaccination (Ahmed et al. 2015; Bisiaux et al., 2017; Moliva et al., 2017; Kroon et al., 2018; Ahmed et al., 2021).

In the lymph node, adaptive immune responses are triggered after dendritic cells present the BCG antigen to $CD4^+$ and $CD8^+$T cells. $CD4^+$T cells reduce the bacterial burden in the lungs and spleen, whereas $CD8^+$T cells prevent extrapulmonary dissemination by killing infected cells (Ahmed et al., 2021). By 8–12 weeks BCG post-vaccination, $CD4^+$T cells include Th1, Th17, Tregs and regulatory Th17 cells, whereas $CD8^+$T cells include cytotoxic and Tregs are expressed. Besides that, B cells differentiate into plasma cells, producing antibodies (Dockrell & Smith, 2017; Shen & Chen, 2017; Xu et al., 2019; Ahmed et al., 2021; Singh et al., 2022). The main immune responses generated after BCG vaccination are summarized in Figure 2.1 and Table 2.1.

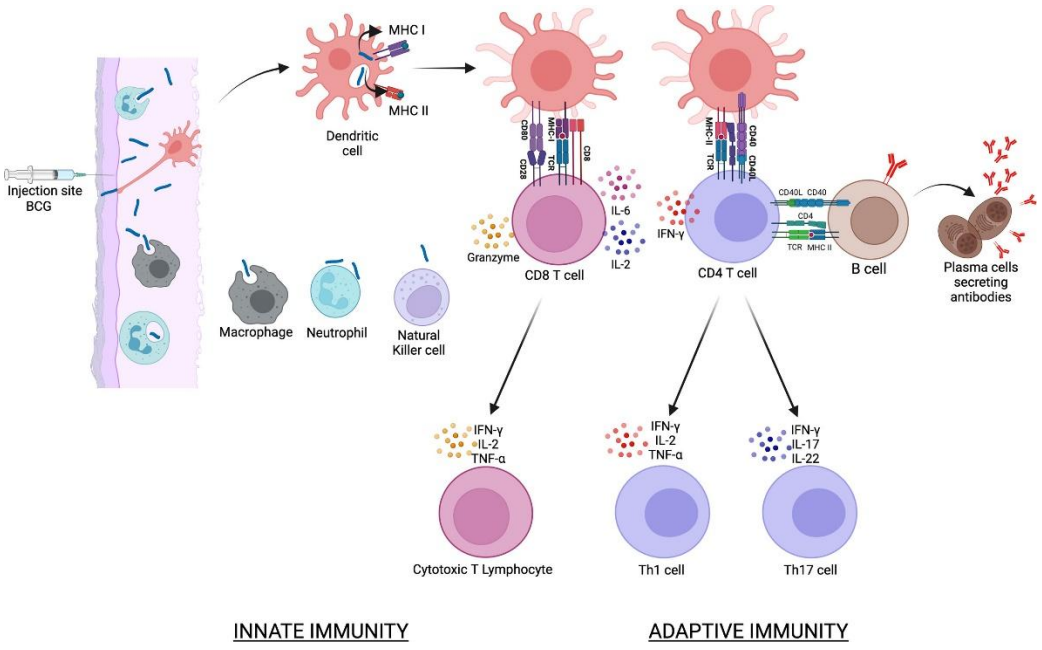

Figure 2.1 The immune responses after intradermal BCG injection. Innate immune cells like dendritic cells, macrophages and neutrophils phagocytose BCG. Dendritic cells present BCG antigens to $CD4^+$ and $CD8^+$ T cells via MHC II and I molecules, respectively, activating B cells, cytotoxic T cells and Th17 cells, forming the adaptive immune response (Sing et al., 2022).

Table 2.1 Summary of immune responses generated after BCG administration

Type of Immune cells	Roles	Releases	References
Macrophages (Innate)	Antigen-presenting cells provide a specialized environment for mycobacteria survival and replication in phagosomes. Gets activated after exposure to BCG resulting in mycobacterial killing by phagosome-lysosome fusion.	Reactive Oxygen Species (ROS), Reactive Nitrogen Intermediates (RNI), TNF-α, IL-12 and IL-6	(Ahmed et al., 2015; 2021)
Neutrophils (Innate)	First immune cell to traffic to the site of infection. Internalize mycobacteria or BCG and eliminate them by ROS or phagolysosome fusing and releasing anti-microbial peptides. Transport internalized BCG to lymph nodes for dendritic cells and T cells to amplify the immune response	IL-1α, IL-1β, IL-8, MIP-1α, MIP-1β, GRO-α, TGF-β, MCP-1, IL-2Rγ, IL-10Rα, and IL-6R	(Bisiaux et al., 2017; Kroon et al., 2018; Ahmed et al., 2021)
Dendritic cells (Innate)	Acts as a link between innate and adaptive response after BCG vaccination, transporting processed antigens to draining lymph nodes for presentation to T cells.	IL-10, IL-4	(Moliva et al., 2017; Ahmed et al., 2021)
T cells $CD4^{+}$Th1 (Adaptive)	IFN-γ is the benchmark for assessing protective immunity induced by BCG	IFN-γ, IL-2 and TNF-α	(Dockrell & Smith, 2017; Singh et al., 2022)
T cells $CD4^{+}$Th17 (Adaptive)	Contributes to either protection against MTB or tissue damage and lung pathology. IL-17A controls inflammation and MTB containment in the lung, but excessive IL-17A can increase inflammation resulting in lung damage and uncontrolled MTB proliferation	IL-17A, IL-23, IL-22, IFN-γ	(Shen & Chen, 2017; Ahmed et al., 2021; Singh et al., 2022)

Table 2.1 Continued

T cells CD8+ Cytotoxic (Adaptive)	Prevents extrapulmonary dissemination	IFN-γ, IL-2 and TNF-α	(Ahmed et al., 2021; Singh et al., 2022)
B cells (Adaptive)	Upon activation by antigen, B cells expand and differentiate into plasma cells secreting antibodies	Antibodies	(Ahmed et al., 2021; Bitencourt et al., 2022; Singh et al., 2022)

2.4.1 BCG Vaccine Effectiveness

BCG is the only vaccine available for preventing TB in children, although its efficacy wanes with age (Fatima et al., 2020). BCG fails to protect against pulmonary TB due to several reasons, including interference with coinfections from environmental mycobacteria and differences in the immune response at the site of the vaccination vs the lungs. Besides that, BCG may have limited efficacy against diverse clinical MTB strains. Challenges also include inadequate animal models and poor translation of *in vitro* findings to *in vivo* outcomes (Moliva et al., 2017; Ahmad et al., 2021). Other factors affecting BCG effectiveness include host genetics, geography, malnutrition and socioeconomic conditions (Kumar, 2021).

2.4.2 Candidate vaccine against TB

Due to the limited efficacy of BCG, researchers are actively developing new TB vaccine candidates, aiming to replace BCG or enhance its protective efficacy (da Costa et al., 2024). According to the World Health Organization, 2024, 15 vaccine candidates are currently in clinical development (World Health Organization, 2024b). Among these, GamTBvac, VPM1002 and M72/AS01E are vaccine candidates that have reached Phase 3 clinical trials (da Costa et al., 2024, World Health Organization, 2024b).

GamTBvac is a recombinant TB vaccine containing MTB antigens ESAT6, CFP10 and AG85A fused with a dextran-binding domain. This vaccine has demonstrated the ability to induce high levels of antigen-specific IFN-γ, Th1 cytokines and IgG antibodies in BCG-immunized adults (Vasina et al., 2019; Tkachuk et al., 2020).

VPM1002 is a live attenuated recombinant vaccine genetically modified to be more efficacious and safer than BCG in young adults and newborns (Nieuwenhuizen

et al., 2017; Kaufmann, 2020). This modification replaces the urease C gene with *Listeria monocytogenes* listeriolysin, resulting in enhanced Th1 and Th17 type immune responses. In BCG, urease C contributes to mycobacteria's survival by neutralizing the phagosomes. However, in VPM1002, the removal of the urease C and the presence of listeriolysin promote phagolysosome fusion, enabling antigen release and triggering autophagy and apoptosis, thereby boosting bacterial clearance (Nieuwenhuizen et al., 2017; Renteria-Flores et al., 2024).

M72/AS01E is a protein subunit vaccine composed of highly immunogenic MTB proteins Mtb32A and Mtb39A combined with AS01E adjuvant (da Costa et al., 2024). These components induce strong humoral and $CD4^+$ T cell responses and are clinically safe in adolescents and adults (Ji et al., 2019; da Costa et al., 2024).

In some TB vaccine candidates, additional adjuvants are required to strengthen the adaptive immune response (Enriquez et al., 2021). For example, in GamTBVac, the Dextran-CpG adjuvant enhances vaccine uptake by antigen-presenting cells. Similarly, in the AEC/BC02 vaccine, currently in Phase IIa clinical trials, aluminium serves both as an adjuvant and delivery system, activating the innate immune response via TLR9 receptor-mediated signalling (da Costa et al., 2024, World Health Organization, 2024b). With promising candidates in clinical trials, ongoing research aims to develop vaccines that are affordable and can be used in various vulnerable populations affected by TB (Junqueira-Kipnis et al., 2024).

2.5 Mycobacteria

Mycobacteria are common environmental bacteria with most species found in soil or water but some are significant human pathogens (Bachmann et al., 2020). The genus *Mycobacterium* comes under the phylum Actinobacteria and belongs to the

Mycobacteriaceae family. The acid-fast organisms in this genus contain mycolic-acid and lipid-rich cell walls, making them resistant to decolorization by acid alcohol (Vilcheze & Kremer, 2017). The organisms in this genus are aerobic to microaerophilic, with slightly curved or straight rods, non-motile and not able to produce spores (Pereira et al., 2020). Mycobacteria are classified as slow or rapid growers based on their *in vitro* growth rates. Slow growers typically take more than seven days to form colonies and are associated with pathogenicity and intracellular lifestyles, whereas rapid growers form colonies within two to five days and are primarily environmental, with some being opportunistic pathogens (Bachmann et al., 2020; Pereira et al., 2020). The colonies are described as either buff, referring to white or cream-colored colonies, or chromogens, characterized by yellow to orange pigmentation depending on light exposure (Forbes et al., 2018; Pereira et al., 2020; Saxena et al., 2021). Löwenstein-Jensen solid egg-based medium and Middlebrook 7H10, Middlebrook 7H11 agar-based mediums are commonly used for culturing mycobacteria, with the later requiring 5 -10% CO_2 for mycobacteria growth (Forbes et al., 2018).

Mycobacteria species can be divided into three main groups; 1) mycobacteria that causes tuberculosis (TB) *M. tuberculosis*, 2) mycobacteria that causes leprosy *M. leprae* and 3) non-tuberculous mycobacteria (NTM) or referred to as environmental mycobacteria (Gopalaswamy et al., 2020; Saxena et al., 2021). *M. tuberculosis* and *M. leprae* are the causes of tuberculosis and leprosy, respectively, but opportunistic infections caused by NTMs are increasingly being reported (Pereira et al., 2020). The most common pulmonary NTM infections are caused by *Mycobacterium avium* complex and *Mycobacterium abscessus*. Their ability to persist on medical devices and

healthcare surfaces highlights their rising importance in human health (Faria et al., 2015).

2.5.1 *Mycolicibacterium smegmatis*

Mycolicibacterium smegmatis (previously *Mycobacterium smegmatis* (MSMEG) classified as a non-tuberculous mycobacterium (NTM), is well-known for its rapid growth, forming colonies within three days and its non-pathogenic nature (Saxena et al., 2021; Sparks et al., 2023). MSMEG initially appears velvety white with fine wrinkles, but it turns into non-pigmented velvety yellow after 48 hours (Sundarsingh et al., 2020; Xie et al., 2023). This bacterium has facilitated the development of genetic tools and facilitated studies on MTB properties, fundamental biological mechanisms and drug targets easily compared to the slow-growing, highly pathogenic MTB (Sparks et al., 2023).

It is noteworthy that over 2800 orthologous protein-coding genes exist in MSMEG, with 96% of essential genes in MSMEG having homologs in MTB. Furthermore, 90% of these homologous genes are crucial for the survival of MTB, proving that MSMEG is a useful model for studying MTB (Xie et al., 2023). *Mycobacterium smegmatis* was renamed *Mycolicibacterium smegmatis* based on molecular markers present in the genomes of the specific groups of mycobacteria (Gupta et al., 2018). However, most researchers continue to use the conventional genus name to avoid confusion in healthcare settings, as changing it would require time-consuming re-education of healthcare professionals and could pose risk to patient safety (Sparks et al., 2023).

M. smegmatis has been extensively studied as a model for biofilm research (Bhunu et al., 2017). MSMEG forms pellicle biofilms at solid-air interfaces (Pereira et al., 2020). The extracellular polymeric substances (EPS) produced by MSMEG, are

crucial to form a biofilm scaffold and consist of mycolic acids that are synthesized in greater amounts in the presence of antibiotics. This adaptation aids the survival of persister cells within biofilms. Furthermore, iron deficiency results in an overexpression of genes related to mycobactin and exochelin biosynthesis, enabling the bacterium to scavenge iron from its environment to support biofilm development (Faria et al., 2015; Pereira et al., 2020).

Beyond biofilm research, MSMEG has demonstrated potential as a vaccine vector, particularly for HIV/AIDS or immunocompromised individuals, due to its non-pathogenic nature (Kannan et al., 2020). Advances in omics, particularly comparative genomics, have revealed significant genetic homology between MSMEG and MTB, underscoring its value as a model for vaccine research (Sundarsingh et al., 2020; Xie et al., 2023). Early studies demonstrated that MSMEG cell wall components can trigger cross-reactivity against MTB antigens in mice. This led to research focused on expressing MTB-specific antigens on MSMEG surface to enhance its immunogenicity as a vaccine vector (Xie et al., 2023).

Research has also shown that recombinant MSMEG with ESX-3 gene deletion enhances immune activation and reintroduction of MTB ESX-3 gene into this recombinant MSMEG vector resulted in greater protection than BCG vaccine (Xie et al., 2023). MSMEG expressing AG85B epitopes also boosts IgG levels in mice (Kadir et al., 2016). Based on its current success and antigenicity, recombinant MSMEG vaccines may soon be developed and licensed for both preventive and therapeutic applications (Xie et al., 2023).

2.6 Extracellular vesicles

Extracellular vesicles (EVs) are nano to micro-sized membrane-bound, lipid bilayer particles that cannot replicate independently and are released by all cell types. Studies on EVs as potential biomarkers and therapeutic tools have been consistently rising over the years due to the unique characteristics of EVs that can reflect the state of the originating cells, while also altering the function and phenotypes of receiving cells (Welsh et al., 2024). Lipids, nucleic acids such as miRNA, mRNA, DNA and proteins are selectively incorporated into the EVs before they get released by the cells (Qin et al., 2020; Lyu et al., 2022).

EVs are classified based on their size, shape, cellular origin, biogenesis and function (Mehaffy et al., 2022). For example, exosomes ranging from 30 - 150 nm are formed in eukaryotic cells by exocytosis whereas ectosomes or microparticles ranging from 100 – 500 nm are released from eukaryotic cells by budding. Apoptotic bodies range from the sizes 1000 nm -5000 nm. On the other hand, prokaryotic EVs, termed microvesicles, range from 20 - 1000 nm and are formed by budding in Gram-negative bacteria. The mechanism of EV formation in Gram-positive bacteria, fungi and mycobacteria are still not clearly understood due to their thick walls (Wang et al., 2019; Qin et al., 2020; Lyu et al., 2022). The International Society for Extracellular Vesicles (ISEV) recommends the generalized usage of the term EVs instead of inconsistent terms related to biogenesis pathways through the minimal information for studies of extracellular vesicles (MISEV 2023) guidelines (Welsh et al., 2024).

EVs from bacteria and fungi play many significant roles in microbial interactions and disease pathogenesis. For example, *P. aeruginosa* transports Pseudomonas Quinolone Signals (PQS) through EVs to interact with other bacteria via lipopolysaccharides, contributing to biofilm formation (Cooke et al., 2020). Besides

that, *P. aeruginosa* EVs also deliver murein hydrolase enzymes to kill other competing bacteria and carry toxins to induce cytotoxicity in human bronchial epithelial cells (Kim et al., 2015). Similarly, fungal EVs such as those from *Cryptococcus neoformans* also showed enhanced pathogenesis in fungal brain infections (Woith et al., 2019). Importantly, EVs have also been detected in human patient samples and tissue biopsies, highlighting their role as potential causative agents in infectious diseases and their utility as diagnostic and vaccine targets (Woith et al., 2019; Jnana et al., 2023).

2.6.1 Extracellular vesicles isolation, characterization and stability

Developing EV-based diagnostics and therapies requires standardized and efficient isolation methods (Pariset et al., 2017). Each isolation method differs in purity, required sample volume and processing time. The choice of EV isolation techniques depends on the characteristics of the EVs such as their size, buoyant density, solubility, physicochemical interactions, protein expression and their intended application (Pariset et al., 2017; Konoshenko et al., 2018). Table 2.2 presents a summary of widely used EV isolation methods and their respective advantages and disadvantages.

Ultracentrifugation is commonly used for EV isolation due to its cost-effectiveness and ability to process large volumes without added chemicals (Shami-shah et al., 2023). This method relies on buoyant density with sequential centrifugation to remove dense non-EVs contaminants. EVs are then pelleted at 100, 000 – 200, 000 × g for two hours, resuspended and recentrifuged to eliminate non-EV proteins (Pariset et al., 2017; Shami-shah et al., 2023). A limitation of ultracentrifugation is the potential of co -purification of bacterial components and other contaminants (Mohammadzadeh et al., 2021; Saint-Pol & Culot, 2025). To improve purity, final purification may include filtration through selective pore microfilters to eliminate residual non-EV

impurities (Prados-Rosales et al., 2011; Konoshenko et al., 2018). The MISEV 2023 guidelines recommend reporting the ultracentrifugation parameters such as speed, rotor type, time, tube type, sample volume and temperature to ensure reproducibility and accurate interpretation of EV isolation results (Welsh et al., 2024).

Table 2.2 Summary of EVs isolation techniques, advantages and limitations

EV isolation methods	Principle	Advantage	Disadvantage	Reference
Differential centrifugation + ultracentrifugation	Low-speed centrifugation removes large particles and ultracentrifugation pellets EVs.	Gold standard. Widely used standard method.	Expensive, time consuming, co purifies with bacterial components, may damage EVs	(Mohammadzadeh et al., 2021; Saint-Pol & Culot, 2025)
Density- gradient centrifugation	Separates EVs based on buoyant density gradient using sucrose or iodixanol.	Improves EV purity for complex samples.	Long isolation time, low yield of high purity material (density-based), Cannot separate EVs from particles with similar density	(Mohammadzadeh et al., 2021; Zhao et al., 2021; Welsh et al., 2024; Saint-Pol & Culot, 2025)
Size exclusion chromatography (SEC)	Separates particles by size using porous matrix; larger particles elute first and smaller particles elute later.	Simple. Columns can be homemade or purchased. High purity, scalable for clinical use.	Dilutes samples, requiring extra concentration steps. Low yield. Needs specialized equipment	(Welsh et al., 2024; Saint-Pol & Culot, 2025)
Immuno-affinity capture	EVs captured through antibody antigen interactions.	High specificity. Captures specific EV subtypes	Costly. May not recover all EV subtypes. Residual antibodies on EVs. Inconsistent yield. Limited specificity when using common EV markers.	(Zhao et al., 2021; Welsh et al., 2024; Saint-Pol & Culot, 2025
Polyethylene Glycol (PEG) Precipitation	PEG reduces EV solubility, causing precipitation at low spin speeds	Simple and cost effective. No extensive equipment required.	Low purity. Precipitates EVs with contaminants	(Zhao et al., 2021; Welsh et al., 2024; Saint-Pol & Culot, 2025

EV characterization requires multiple methods as no universal marker or technique exists (Hartjses et al., 2019; Welsh et al., 2024). Recent literature reported approaches such as biochemical colorimetric assays to determine the total protein concentration, transmission electron microscopy (TEM) to verify EV structure, nanoparticle tracking analysis (NTA) to measure EV concentrations and size distribution and immunoblotting for EV markers (Hartjes et al., 2019; Lyu et al., 2022; van de Wakker et al., 2022; Walker et al., 2022). Despite the availability of multiple techniques, each method has its limitation that can affect the data interpretation. For example, imaging approaches may alter EV morphology during sample preparation, size-based methods can be biased by sample heterogeneity and protein-based assays cannot distinguish between EV subtypes or contaminants. Therefore, combining complementary methods is recommended to obtain a comprehensive reliable characterization of EVs. Table 2.3 summarizes the principles, advantages and limitations of commonly used EV characterization methods.

Table 2.3 Summary of EVs characterization techniques, advantages and limitations

EV characterization methods	Principle	Advantage	Disadvantage	Reference
Direct imaging				
Transmission Electron Microscopy (TEM)	Uses a beam of electrons to create an image of the studied samples.	High resolution imaging. Can detect EVs of all sizes and can measure EV diameter.	Requires fixation/ dehydration. Preparation may alter EV structure. Low throughput	(Szatanek et al., 2017; Welsh et al., 2024)
Atomic Force Microscopy (AFM)	A probe tip scans the sample surface and the deflections are detected by a laser to generate 3D image	Label or stain free. Shows size and ultrastructure. Measure nanomechanical properties.	Surface binding may alter EVs. Low throughput. Requires specialized equipment or expertise. High cost.	(Szatanek et al., 2017; Zhao et al., 2021; Welsh et al., 2024)
Indirect imaging				
Dynamic Light Scattering (DLS)	Measures fluctuation in scattered laser light to calculate particle diffusion and hydrodynamic size	Fast and simple. Gives average size and polydispersity. Suitable for routine analysis.	Works best for uniform samples but not ideal for complex fluids. Limited resolution.	(Hartjes et al., 2019; Welsh et al., 2024; Saint-Pol & Culot, 2025)
Tunable Resistive Pulse Sensing (TRPS)	Particles pass through a size adjustable nanopore, temporarily blocking the current. The pulse size gives particle size, concentration and surface charge.	Accurate single particle sizing and concentration without DLS bias	Cannot image EVs. Difficult for heterogenous samples.	(Szatanek et al., 2017; Saint-Pol & Culot, 2025)

Table 2.3 Continued

Nanoparticle Tracking Analysis (NTA)	Tracks Brownian motion of individual particles using laser light to calculate size and concentration	Measures individual EV size and concentration	Requires careful dilution. Small volume is challenging. Quantum dot antibodies may cause high background.	(Szatanek et al., 2017; Welsh et al., 2024)
Flow cytometry	Detects light scatter and fluorescence from single particle in a flow	High throughput, analyses surface markers to detect EVs with advanced systems	Expensive. Require specialized equipment. Poor sensitivity for small EVs. Requires fluorescent labelling for detection of specific markers	(Szatanek et al., 2017; Hartjes et al., 2019)
Fluorescence-based EV analysis	EVs are labelled with lipophilic dyes or fluorescent antibodies. Fluorescent is detected to visualize and analyse markers	High sensitivity. Allows single EVs analysis. Can measure size, concentration and multiple markers	Background from unbound dye. Require specialized equipment. Need further standardization	(Szatanek et al., 2017; Hartjes et al., 2019)
Biochemical analysis				
Total protein concentration (Micro-bicinchoninic acid (BCA) or Bradford assay)	Measures total or specific protein concentration in EVs using colorimetric assay	Simple. Can quantify total protein.	Needs purified EVs. Cannot differentiate EV subtypes	(Hartjes et al., 2017; van de Wakker et al., 2022)
Western Blotting	Detects specific EV proteins using antibodies	Identifies EV specific markers. Confirms sample purity	Potential for non-specific signal.	(Lyu et al., 2022; Saint-Pol & Culot, 2025)

Scalable EV production for therapeutic use requires understanding factors that affect EV stability and recovery. Storage temperature affects EV size, morphology, and yield, with -80°C preserving EV properties, while 4°C and -20°C reduced EV number, size and antibacterial activity (van de Wakker et al., 2022). However, -80°C storage poses challenges due to transportation limitations, higher costs and the need for cold chain maintenance from production to patient use (Jeyaram & Jay, 2017; Richter et al., 2019). The use of disaccharide stabilizers such as trehalose in EV storage buffers as cryoprotectants prevents protein aggregation during freezing (Jeyaram & Jay, 2017; Richter et al., 2019). Lyophilization with trehalose also maintains EV markers, protein and RNA profiles as compared to fresh EVs (Richter et al., 2019; Qin et al., 2020). This approach addresses stability and storage challenges without relying on -80°C storage. MISEV 2023 also recommends that researchers standardize their storage protocol and minimize freeze-thaw cycles through careful aliquoting (Welsh et al., 2024). Improving isolation, characterization and storage methods will support scalable EV production for therapeutic applications.

2.6.2 Mycobacteria EVs

Mycobacteria EVs were first identified within the extracellular matrix of *Mycobacterium ulcerans* biofilms and were isolated from biopsies of Buruli ulcer-like lesions in infected mice tail tissues (Marsollier et al., 2007; Rodriguez & Prados-Rosales, 2016; Gupta & Rodriguez, 2018; Mehaffy et al., 2022). EVs were also discovered in the culture supernatants of both pathogenic and environmental mycobacterial species including *M. tuberculosis*, *M. bovis* BCG, *Mycobacterium kansasii*, *Mycobacterium avium*, *Mycobacterium avium* subspecies *paratuberculosis*,